Grain-boundary-induced spin disorder in nanocrystalline gadolinium

2009 J. Phys.: Condens. Matter 21 156003

(http://iopscience.iop.org/0953-8984/21/15/156003)

J. Phys.: Condens. Matter **21** (2009) 156003 (5pp) doi:10.1088/0953-8984/21/15/156003

Grain-boundary-induced spin disorder in nanocrystalline gadolinium

F Döbrich[1,4], M Elmas[1], A Ferdinand[1], J Markmann[1], M Sharp[2], H Eckerlebe[2], J Kohlbrecher[3], R Birringer[1] and A Michels[1]

[1] Technische Physik, Universität des Saarlandes, D-66041 Saarbrücken, Germany
[2] GKSS Forschungszentrum, D-21502 Geesthacht, Germany
[3] Paul Scherrer Institute, CH-5232 Villigen PSI, Switzerland

E-mail: f.doebrich@nano.uni-saarland.de

Received 16 February 2009, in final form 27 February 2009
Published 20 March 2009
Online at stacks.iop.org/JPhysCM/21/156003

Abstract
Based on experimental magnetic-field-dependent neutron scattering data, we have calculated the autocorrelation function of the spin misalignment of nanocrystalline ^{160}gadolinium. The analysis suggests the existence of two characteristic length scales in the spin system: the smaller one is about 5 nm and is attributed to the defect cores of the grain boundaries, whereas the larger length scale is of the order of the average crystallite size $D = 21$ nm and presumably describes the response of the magnetization to the magnetic anisotropy field of the individual crystallites.

1. Introduction

The magnetic properties of a solid are largely influenced by the geometry and topology of the building units of its microstructure. In the ever-growing field of nanomagnetism, this rationale is exploited by continuously developing sophisticated fabrication procedures for synthesizing advanced nanostructures, which range from complex bulk materials to a broad variety of low-dimensional systems [1–3]. However, not only the geometry and spatial arrangement of the building units determine the magnetic behavior but also lattice imperfections such as internal or external interfaces, phase boundaries or topological defects have an impact on magnetism.

An important class of materials where defects are expected to have a strong influence on magnetic properties are the rare-earth metals [4]: it is mainly the position-dependent RKKY exchange interaction along with their extremely large magnetostriction which should render magnetism in these 4f systems sensitive to structural disorder and imperfections. In fact, in a number of recent experiments, mostly on heavy rare-earth metals, it was demonstrated that the symmetry breaking, which is associated with interfaces, plays a dominant role for magnetic property changes when compared to the respective quasi-zero-disorder reference states (see, e.g., [5–16] and references therein). Particularly remarkable is the polarized-neutron experiment by Grigoriev *et al* [17], who have shown that an external magnetic field can induce a preferred chirality in the helix structure of a Dy/Y multilayer system, the origin of which was attributed to the broken symmetry at the interfaces.

Our interest is focused towards understanding the effect of internal interfaces (grain boundaries) in nanocrystalline (nc) bulk Gd on its magnetic microstructure. In [18], we have reported the first magnetic small-angle neutron scattering (SANS) study on nc Gd, which was synthesized using the low neutron-capturing isotope ^{160}Gd. Note that, due to its enormous capture cross section for thermal neutrons, only a very few neutron studies on bulk Gd exist (e.g. [19–23]). One of the central results of [18] is the observation of a clover-leaf-type angular anisotropy in the magnetic SANS cross section, which has been rationalized in terms of correlated nanoscale longitudinal and transversal spin fluctuations. The origin of the longitudinal fluctuations was attributed to the atomic-site disorder which is located in the core region of the grain boundaries.

It is the purpose of this report to provide independent evidence for the relevance of grain boundaries in nc Gd by analyzing the field-dependent SANS data in terms of the autocorrelation function of spin misalignment. From this type of analysis, we are able to estimate the characteristic range over which grain boundaries in nc Gd perturb the spin distribution.

2. Experiment

Synthesis of nc Gd was carried out by the inert-gas condensation technique, as described, for example, in [8].

[4] Author to whom any correspondence should be addressed.

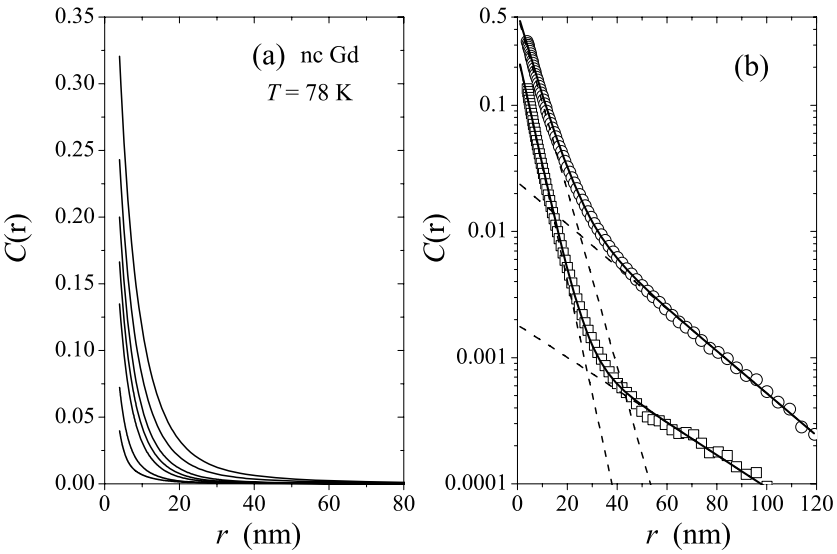

Figure 1. (a) Correlation function $C(r)$ of the spin misalignment of nanocrystalline (nc) ^{160}Gd at $T = 78$ K. $C(r)$ was computed using equation (1). Average crystallite size of the nc Gd sample is $D = 21$ nm. Values of the applied magnetic field from top to bottom (in mT): 0, 10, 30, 60, 100, 300, 600. (b) $C(r)$ from (a) on a log-linear scale at 0 mT (open circles) and 100 mT (open squares). It is seen that $C(r)$ contains two characteristic length scales, as indicated, respectively, by the dashed lines. Solid lines: fit to equation (2) subject to the constraint $C_1 + C_2 = C(r = 0)$.

The low-capturing isotope ^{160}Gd (enrichment: 98.6%) was used as a starting material in the evaporation process. The average crystallite size of the nc Gd sample was determined by analysis of x-ray diffraction data and found to be $D = (21 \pm 6)$ nm [24, 25]. The mass density of conventional nc Gd, which is prepared under the same experimental conditions as the present nc ^{160}Gd specimen, is typically 99% of bulk [8]; this suggests the absence of pore scattering [26, 27]. The SANS experiments were performed at the SANS I instrument at the Paul Scherrer Institute, Switzerland, and at SANS 2 at the Geesthacht Neutron Facility, Germany. Magnetization measurements were carried out on conventional Gd in a Quantum Design PPMS magnetometer. For further details, see [18].

3. SANS data analysis and results

The SANS data analysis is based on the autocorrelation function $C(r)$ of spin misalignment [10, 28]. At a given magnetic field, $C(r)$ contains information on the characteristic length scales over which gradients in the magnetization are correlated. The function $C(r)$ is related to the radially averaged spin-misalignment scattering cross section $\mathrm{d}\Sigma_\mathrm{M}/\mathrm{d}\Omega$ according to [10, 28]

$$C(r) = \frac{K}{r} \int_0^\infty \frac{\mathrm{d}\Sigma_\mathrm{M}}{\mathrm{d}\Omega}(q) \sin(qr) q \, \mathrm{d}q, \qquad (1)$$

where K is a constant. $\mathrm{d}\Sigma_\mathrm{M}/\mathrm{d}\Omega$ was obtained from the total unpolarized SANS cross section $\mathrm{d}\Sigma/\mathrm{d}\Omega$ (see figure 3 in [18]) by subtracting the residual nuclear and magnetic scattering cross section $\mathrm{d}\Sigma_\mathrm{R}/\mathrm{d}\Omega$, which is measured at complete saturation. As an approximation to $\mathrm{d}\Sigma_\mathrm{R}/\mathrm{d}\Omega$, the SANS data measured at the highest applied field of 5 T were used.

The autocorrelation function $C(r)$ at several applied fields and at $T = 78$ K is displayed in figure 1(a). Similar to nc Ni and Co [28], $C(r)$ is a monotonically decaying function of the distance r, and an increase of the applied field results in the suppression of the magnitude of spin-misalignment fluctuations and in an overall decrease of the range of the correlations. Closer inspection of the $C(r)$ data suggests the existence of at least two characteristic length scales in the spin system (compare figure 1(b)). In order to extract these characteristic length scales, we have analyzed the correlation function (at a particular field) by a sum of two decaying exponentials[5]:

$$C(r) = C_1 \exp(-r/L_1) + C_2 \exp(-r/L_2), \qquad (2)$$

where L_1 and L_2 denote the spin-misalignment lengths, which can be taken as a measure for the characteristic distance over which spin inhomogeneities decay. The value of the correlation function at the origin, $C(r = 0) = C_1 + C_2$, is by definition identical to the mean-square magnetization fluctuation [10, 28].

In order to roughly estimate the errors in L_1 and L_2, we have analyzed different schemes for extrapolating the SANS data beyond the limits of measurement to $q = 0$ and to $q \to \infty$. Besides the error which is involved in the Fourier transformation procedure, equation (1), there is an additional source of error which results from subtracting the highest-field SANS data, which are used to approximate the residual scattering cross section $\mathrm{d}\Sigma_\mathrm{R}/\mathrm{d}\Omega$ from the measurements at lower fields. Taking all these sources of error into account,

[5] Note that we have previously [18] reported a *single* spin-misalignment length l_C, which was identified with the r value for which the correlation function $C(r)$ decays to $\exp^{-1}$ of its value at the origin $C(r = 0)$. Since such a definition for l_C puts emphasis on the region of the smallest r, the l_C values reported in [18] should be compared with L_1 only.

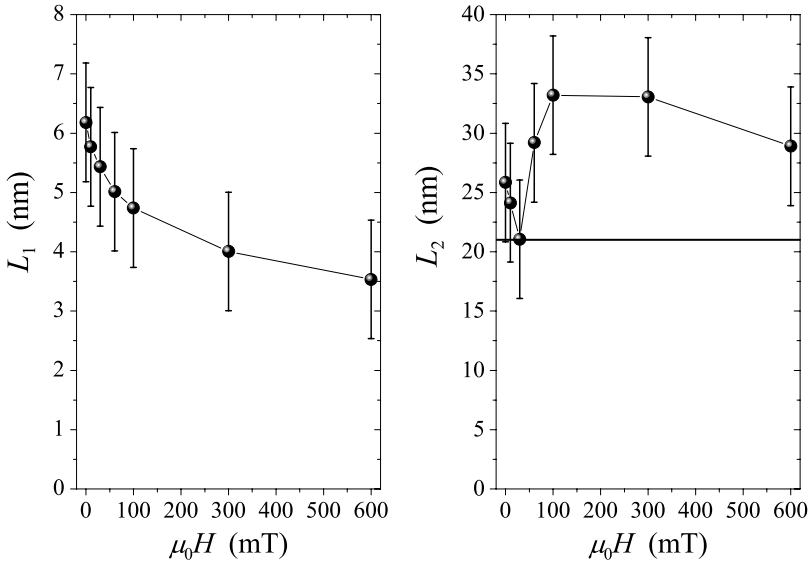

Figure 2. (●) Field dependence of the correlation lengths of spin misalignment L_1 and L_2 of nanocrystalline ^{160}Gd. L_1 and L_2 were obtained by fitting equation (2) to the $C(r)$ data from figure 1(a). Lines are guides to the eye. Solid horizontal line: average crystallite size D of the nc ^{160}Gd sample, which corresponds to the ratio of the fourth to the third moment of a lognormal grain-size distribution [24].

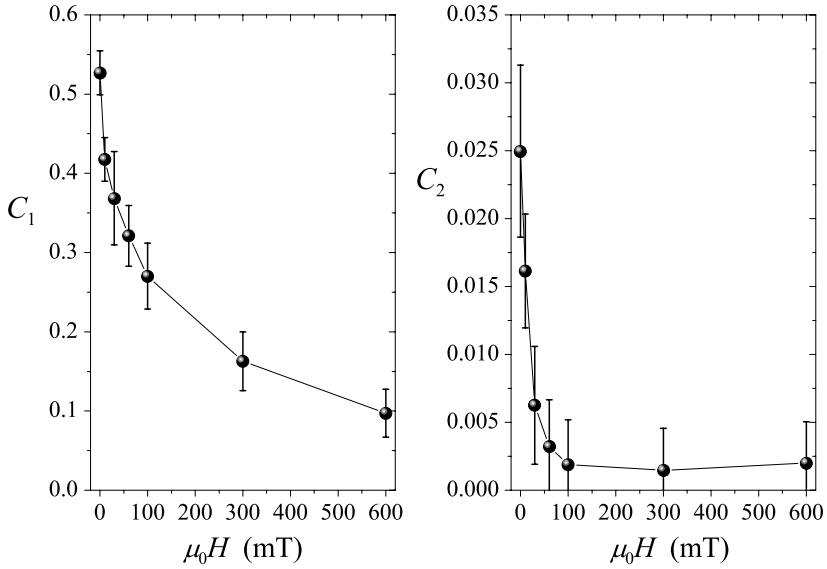

Figure 3. (●) Field dependence of C_1 and C_2. C_1 and C_2 were obtained by fitting equation (2) to the $C(r)$ data from figure 1(a). $C_1 + C_2$ is equal to the normalized mean-square magnetization fluctuation. Lines are guides to the eye.

we find that L_1 and L_2 vary, respectively, within ± 1 nm and ± 5 nm.

Figures 2 and 3 depict, respectively, the results for the field dependences of L_1 and L_2 and of C_1 and C_2. It is seen that L_1 ranges from 4 to 6 nm, which is about five times the structural width of a grain boundary [29] but significantly smaller than the grain size of the nc Gd sample, $D = 21$ nm. The length scale L_1 as well as the weight C_1 of this contribution to the mean-square magnetization fluctuation decrease with increasing applied field. In agreement with the observation of the clover-leaf-type anisotropy in the SANS signal of nc Gd [18], which has been explained with the existence of a jump in the magnetization **M** at grain boundaries, it seems plausible to relate the short-range length scale L_1 and the corresponding C_1 to the defect character of the grain boundaries. The atomic-site mismatch (disorder) that is localized in the grain-boundary core of width $\sim$1 nm seems to induce spin misalignment which is transmitted by the exchange interaction into the interior of the adjacent crystallites. Obviously, the grain-boundary core is decorated by a gradient in **M** which decays within L_1.

Since the exchange integral in Gd depends sensitively on interatomic distances [30, 31], the atomic-site disorder at internal interfaces may also give rise to exchange-weakened bonds or even to antiferromagnetic couplings. Such a scenario [32] may then explain, at least partly, the reduction of the Curie transition temperature in bulk Gd at small crystallite size [8].

The second length scale L_2 varies between about 25 and 35 nm and its weight C_2 decreases with increasing applied field by about an order of magnitude. Correlating L_2 with an

additional but different regime of spin misalignment requires identifying an additional and plausible source of spin disorder. We assign the random magnetic anisotropy which is present in the bulk of the Gd grains to manifest the second source term. For uniformly magnetized grains with discontinuous jumps in the orientation of **M**, the characteristic length scale is expected to be of the order of D, as was found in nc Co [28]. Therefore, it seems plausible that the value of L_2 compares with D (solid line in figure 2). The variation of L_2 with field is beyond what can be explained by our analysis. The observation in figure 2 that $L_2 > D$ should, however, not be seen as an invalidation of the above given argument. In fact, D as obtained by x-ray Bragg-peak-profile analysis represents the ratio of the fourth $\langle D^4 \rangle$ to the third moment $\langle D^3 \rangle$ of a lognormal grain-size distribution [24]. In nuclear particle scattering, the particle size is often determined from the experimental value of the radius of gyration R_G, which for spherical particles of size $2R$ is related to the moments of the distribution according to $(2R)^2 = 20/3R_G^2 = \langle D^8 \rangle / \langle D^6 \rangle$ [33]; evaluation of these integrals assuming a lognormal particle-size distribution with a variance of $\sigma = 1.7$ [24] yields a rigorous upper bound of 56 nm for the particle size. Our values for L_2 are bounded by these two measures for the grain size and, therefore, support our view that L_2 emerges as a consequence of the random magnetic anisotropy of the grains.

Independent support for the interface-induced spin-disorder scenario is provided by magnetization measurements, which were carried out as a function of the average grain size. Figure 4 shows (at $T = 5$ K and $\mu_0 H = 9$ T) the relative reduction of the magnetization, $\Delta M/M$, between coarse-grained and nanoscale Gd for several crystallite sizes. The quantity $\Delta M/M$ scales roughly linearly with D^{-1} (solid line in figure 4), which strongly suggests that the dominant source of spin disorder in nc Gd is related to the grain boundaries, the volume fraction of which is proportional to D^{-1}. This assessment is further supported by taking into account that the parameter C_1, which is supposed to characterize the contribution of the grain boundaries to the mean-square magnetization fluctuation, is at all fields more than one order of magnitude larger than C_2 (compare figure 3).

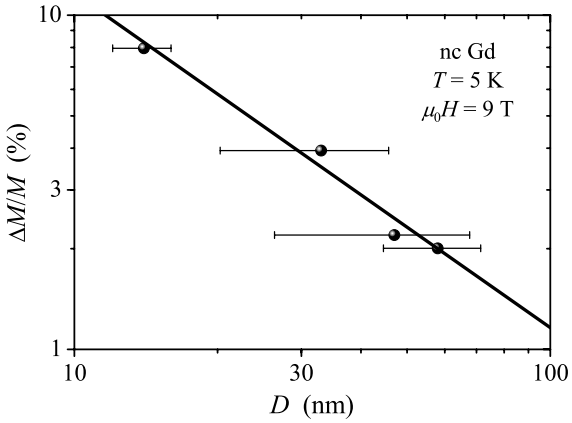

Figure 4. (●) Grain-size dependence of the relative reduction $\Delta M/M$ of the magnetization of conventional nanocrystalline (nc) Gd at $\mu_0 H = 9$ T and $T = 5$ K (log–log scale). $\Delta M/M$ is defined as $(M_{\text{coarse}} - M_{\text{nano}})/M_{\text{coarse}}$, where M_{coarse} is the experimental magnetization of coarse-grained Gd ($D > 100$ nm), which (at 9 T and 5 K) is practically identical to the single-crystal value for the saturation magnetization, $\mu_0 M_S = 2.69$ T [18], and M_{nano} denotes the corresponding magnetization value of nc Gd. Solid line: $\Delta M/M \propto D^{-1}$.

4. Summary

To summarize, we have analyzed magnetic-field-dependent small-angle neutron scattering (SANS) data of nanocrystalline ^{160}Gd by means of the autocorrelation function $C(r)$ of spin misalignment. The results for $C(r)$ indicate the presence of two characteristic length scales in the spin structure. By assuming the correlations to decay exponentially, according to equation (2), we find that $L_1 \cong 5$ nm and $L_2 \cong 25$–35 nm for applied fields between 0 and 0.6 T. In agreement with grain-size-dependent magnetization data and the observation of a clover-leaf-type anisotropy in the magnetic scattering cross section [18], we attribute L_1 to the spin disorder which is caused by the defect cores of the grain boundaries, whereas L_2 is related to the magnetic anisotropy of the individual crystallites. As shown previously [34], for the itinerant band magnets Co and Ni, the atomic-site disorder of grain boundaries is not reflected in an associated spin disorder seen in the SANS signal. In those systems, the random magnetic anisotropy is the dominating source of spin misalignment. However, in nanocrystalline Gd it has now become possible to unravel the spin disorder at/across internal interfaces mediated by the highly position-sensitive RKKY interaction. Overall, the outlined procedure demonstrates the power of the magnetic SANS technique for the quantitative analysis of magnetic microstructures [35].

Acknowledgments

We gratefully acknowledge financial support by the European Commission (contract no. RII-CT-2003-505925), by the Deutsche Forschungsgemeinschaft (grant no. MI 738/3-1) and by the Universität des Saarlandes. We thank Andreas Tschöpe for critically reading the manuscript.

References

[1] Cowburn R P 2000 *J. Phys. D: Appl. Phys.* **33** R1
[2] Skomski R 2003 *J. Phys.: Condens. Matter* **15** R841
[3] Bader S D 2006 *Rev. Mod. Phys.* **78** 1
[4] Legvold S 1980 *Ferromagnetic Materials* vol 1 ed E P Wohlfarth (Amsterdam: North-Holland) pp 183–295
[5] Farle M, Baberschke K, Stetter U, Aspelmeier A and Gerhardter F 1993 *Phys. Rev.* B **47** 11571
[6] Gajdzik M, Trappmann T, Sürgers C and Löhneysen H V 1998 *Phys. Rev.* B **57** 3525
[7] O'Shea M J and Perera P 1999 *J. Appl. Phys.* **85** 4322
[8] Michels D, Krill C E III and Birringer R 2002 *J. Magn. Magn. Mater.* **250** 203
[9] Yan Z C, Huang Y H, Zhang Y, Okumura H, Xiao J Q, Stoyanov S, Skumryev V, Hadjipanayis G C and Nelson C 2003 *Phys. Rev.* B **67** 054403

[10] Weissmüller J, Michels A, Michels D, Wiedenmann A, Krill C E III, Sauer H M and Birringer R 2004 *Phys. Rev.* B **69** 054402
[11] Heigl F, Prieto J E, Krupin O, Starke K, Kaindl G and Bode M 2005 *Phys. Rev.* B **72** 035417
[12] Kruk R, Ghafari M, Hahn H, Michels D, Birringer R, Krill C E III, Kmiec R and Marszalek M 2006 *Phys. Rev.* B **73** 054420
[13] Yue M, Zhang J X, Zeng H and Wang K J 2006 *Appl. Phys. Lett.* **89** 232504
[14] Yue M, Wang K J, Liu W Q, Zhang D T and Zhang J X 2008 *Appl. Phys. Lett.* **93** 202501
[15] Philippi S, Markmann J, Birringer R and Michels A 2009 *J. Appl. Phys.* **105** 07A701
[16] Bataille A M, Dumesnil K, Gukasov A and Dufour C 2009 *J. Appl. Phys.* **105** 07A928
[17] Grigoriev S V, Chetverikov Y O, Lott D and Schreyer A 2008 *Phys. Rev. Lett.* **100** 197203
[18] Michels A, Döbrich F, Elmas M, Ferdinand A, Markmann J, Sharp M, Eckerlebe H, Kohlbrecher J and Birringer R 2008 *Europhys. Lett.* **81** 66003
[19] Will G, Nathans R and Alperin H A 1964 *J. Appl. Phys.* **35** 1045
[20] Cable J W and Wollan E O 1968 *Phys. Rev.* **165** 733
[21] Koehler W C, Child H R, Nicklow R M, Smith H G, Moon R M and Cable J W 1970 *Phys. Rev. Lett.* **24** 16
[22] Moon R M, Koehler W C, Cable J W and Child H R 1972 *Phys. Rev.* B **5** 997
[23] Child H R 1978 *Phys. Rev.* B **18** 1247
[24] Krill C E and Birringer R 1998 *Phil. Mag.* A **77** 621
[25] Markmann J, Yamakov V and Weissmüller J 2008 *Scr. Mater.* **59** 15
[26] Sanders P G, Eastman J A and Weertman J R 1998 *Acta Mater.* **46** 4195
[27] Michels A, Elmas M, Döbrich F, Ames M, Markmann J, Sharp M, Eckerlebe H, Kohlbrecher J and Birringer R 2009 *Europhys. Lett.* **85** 47003
[28] Michels A, Viswanath R N, Barker J G, Birringer R and Weissmüller J 2003 *Phys. Rev. Lett.* **91** 267204
[29] Sutton A P and Balluffi R W 1995 *Interfaces in Crystalline Materials* (Oxford: Clarendon) p 287
[30] Kurz P, Bihlmayer G and Blügel S 2002 *J. Phys.: Condens. Matter* **14** 6353
[31] Turek I, Kudrnovský J, Bihlmayer G and Blügel S 2003 *J. Phys.: Condens. Matter* **15** 2771
[32] Fisher M E and Ferdinand A E 1967 *Phys. Rev. Lett.* **19** 169
[33] Möller J, Kranold R, Schmelzer J and Lembke U 1995 *J. Appl. Crystallogr.* **28** 553
[34] Weissmüller J, Michels A, Barker J G, Wiedenmann A, Erb U and Shull R D 2001 *Phys. Rev.* B **63** 214414
[35] Michels A and Weissmüller J 2008 *Rep. Prog. Phys.* **71** 066501